International Global Navigation Satellite Systems Association
IGNSS Symposium 2020

Colombo Theatres, Kensington Campus, UNSW Australia
5 – 7 February 2020

Celestial Fix as a Generalized Eigenvalue Problem

Hatem Hmam
Defence Science and Technology Group,
Edinburgh, SA 5111, Australia
Email: hatem.hmam@dst.defence.gov.au

ABSTRACT

In this paper a novel algorithm for solving the self-localization problem based on celestial sight reduction is presented. This localization approach uses sightings of several celestial bodies and measurements of their altitudes in the sky to estimate the navigator's position on an ellipsoidal earth. The main advantage of this algorithm is that it transforms the search for the optimal navigator fix into a generalized eigen-decomposition where often, only the largest eigenvalue is of interest. Several high-level languages and programming platforms such as Matlab, readily provide routines that selectively and efficiently solve for the largest or smallest eigenvalue. The last part of the paper presents Monte Carlo simulations using the proposed computation approach and provides performance analysis in terms of star altitude measurement error. Some insight on how to increase localization accuracy is also given.

KEYWORDS: Celestial navigation, Trust region subproblem, Generalized eigenvalues, Geolocation, Passive localization

1. INTRODUCTION

Navigating the globe and the wild seas has long been a challenge for sailors and warriors through history. During the last century the US Department of Defense (DoD) has funded a number of localization related projects, small and large, with an aim to develop mobile positioning sensors or build navigation/positioning infra-structure, both within continental US and abroad. The main initial motive was to enable its large fleet of long range platforms (e.g. intercontinental missiles, spy planes, ships and submarines) to navigate anywhere in the world, knowing where they are at any moment. This mission proved to be challenging to achieve in all-weather conditions and historically a number of technologies have been considered, ranging from relative positioning sensors (i.e. inertial navigation systems) to the currently popular Global Positioning System (GPS).

The ancient technique of tracking specific stars and star constellations in the sky and measuring how high they are (e.g. Polaris) are in the sky, is not forgotten and was implemented in many US long range platforms [1]. This type of navigation is commonly known as celestial navigation and has been practiced for millennia in many parts of the world.

Since 2015, and not very long after celestial navigation has been axed by the US Navy, stellar navigation has regained interest and was re-introduced as part of navy training. The Navy's decision was motivated by the increasing threat of electronic attack and its policy of an independent positioning and timing method (other than GPS).

Star positions are conveniently represented as angle coordinates on a celestial sphere, which is an imaginary sphere centered at the Earth centre and whose North axis coincides with the earth's North pole axis. A graphic illustration of this star positioning method is given in Figure 1. Celestial navigation relies on altitude measurement of known stars/planets whose directions are tabulated in a current 'almanac'. The star altitude or height, which is defined as the star elevation angle above the horizon, is usually measured using a sextant. The altitude measurement time needs to be accurate to the nearest second. A number of altitude corrections (e.g. correction due to refraction of star light while traversing the earth's atmosphere) are usually applied to the raw altitude measurement before it is used for geolocation. The corrected altitude, referred to as the observed altitude, is used to generate a line of position (LOP) around the star geographic position.

An almanac records in great detail the angle positions of most navigation stars and planets during a year. It mainly consists of hourly body angle position tables with respect to a rotating earth. A precise universal time-keeping (Universal Time or UT1) device such as a chronometer is required to convert the local time to the universal time. If UT time is not available, then the Coordinated Universal Time (UTC) may be used instead and results in tolerable body angle position errors. The universal time along with the current date and the star/planet under consideration, are used as an index to a unique table entry in the almanac. If the current time of interest is not an integer number of hours, then interpolation of star direction positions within the hour is carried out. For the sun, moon, planets, and first point of Aries, the direction data is recorded as two angles: the Greenwich Hour Angle (similar to Geodetic longitude but positive westward) and the Declination (similar to Geodetic latitude). For the remaining 57 navigation stars, the star GHA is the sum of the GHA of Aries and the star Sidereal Hour Angle (SHA). The process of generating lines or circles of position for self-localization purposes is referred to as sight reduction.

According to [2], the tabulated GHA and Dec angles display an error of at most $0.2'$ (0.2 arc-minutes), but these errors can be slightly larger for the sun and moon. The GHA error may reach $0.25'$ for the sun and $0.3'$ for the moon. Following [3, Chapter 16], the altitude error standard deviation of a marine sextant is typically around $1'$ and is larger for a bubble sextant. To achieve an accurate geolocation fix, it is recommended [4, Chapter 14 and 18] to select stars from all directions, with an altitude between 30^o and 70^o. This star selection approach helps mitigate the effect of altitude measurement systematic errors and improve localization geometry.

The literature on sight reduction and positioning is diverse and mostly focusses on applying spherical trigonometry to estimate the navigator's location. The classical method of celestial positioning is the altitude intercept method, initially developed by the French navy officer, St. Hilaire, which assumes the availability of an initial position, or assumed position (AP), typically within no more than 100 nautical miles of the true navigator's position, There is a significant amount of literature on sight reduction positioning using this method [3]. Other works do not necessitate prior knowledge of an initial position and provide numerical algorithms to solve the geolocation problem [5]. Chief among these is the approach proposed by Metcalf [6][7], which transforms the geolocation problem into a quadratic optimization

problem with a single quadratic constraint, and provides an exact numerical fix by iteratively solving a rational equation.

The approach followed in the current work is similar to [6] and formulates the localization problem as a Trust Region Subproblem (TRS) [8]. The main difference, however, is the provision of a closed form solution through the computation of a specific generalized eigenpair of the TRS problem [9]. This solution method requires no solution iteration other than that implemented within the built-in eigen-solver.

The layout of this paper is organized as follows. Section 2 provides a brief introduction of the TRS problem and its solution, as applied to the current problem of multi-body celestial-based positioning. The analysis in Section 3 imposes a further constraint such as prior knowledge of the region where the navigator resides. Section 4 presents several Monte Carlo computer simulations and provides some localization performance numbers of interest to navigators and geolocation experts.

2. SIGHT REDUCTION POSITIONING

2.1 Lines of Position

Given an observed star, one first measures its altitude and records the corresponding measurement time (UT time accurate to the nearest second). This time and date are then used to find its geographic position in terms of Greenwich Hour Angle (GHA) and Declination (d),

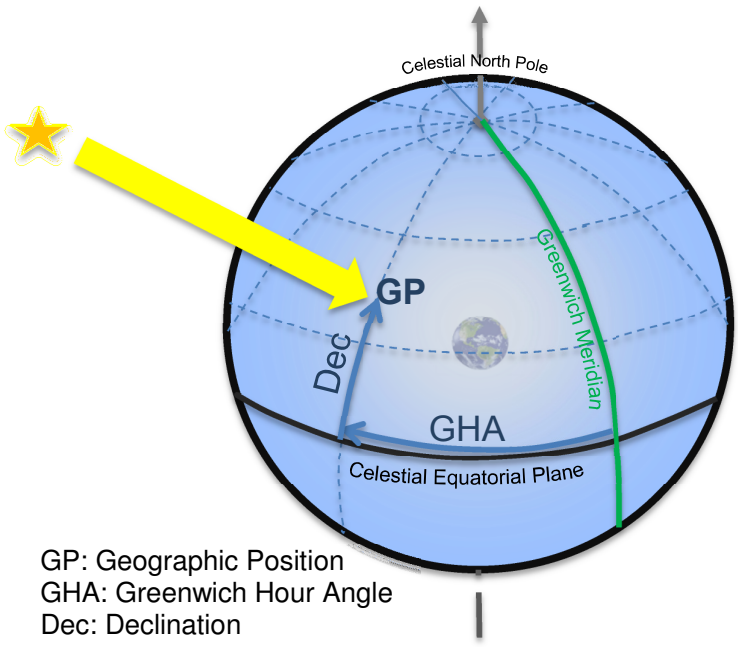

Figure 1. Celestial sphere. Both the celestial North pole and equatorial plane coincide with those of earth. Similar to the Geodetic reference system, the celestial sphere consists of longitudes (positive westward) and latitudes (positive above the celestial equatorial plane).

which are extracted from a current nautical almanac. These two angles are shown in Figure 1 for a star (or planet) whose geographic position occurs on the Northern celestial sphere (positive declination). The direction of a sighted star is represented by the unit vector

$$\boldsymbol{s}_i = \begin{bmatrix} \cos(d_i)\cos(GHA_i) \\ \cos(d_i)\sin(GHA_i) \\ \sin(d_i) \end{bmatrix}$$

where i indexes the ith observed star among n stars.

Let Lon and Lat be the Geodetic Longitude and Latitude of the navigator. The Geodetic vertical is oriented along the unit vector,

$$\boldsymbol{u} = \begin{bmatrix} \cos(Lat)\cos(Lon) \\ -\cos(Lat)\sin(Lon) \\ \sin(Lat) \end{bmatrix},$$

where the minus sign is introduced to reverse the Geodetic longitude to comply with the GHA convention (positive westward). The measured altitude, a_i, corresponding to the ith star, is the angle distance between the horizon and the ith star direction and satisfies in the noiseless case,

$$\boldsymbol{s}_i^T \boldsymbol{u} = \sin\ a_i\ , 1 \le i \le n \tag{1}$$

The ith line of position (LOP) is given by the ith dot product equation (1).

2.2 Trust Region Subproblem (TRS) Formulation

If one vertically stacks all left and right hand sides of the measurement equations (1), one obtains the linear matrix equation

$$G\boldsymbol{u} = h \tag{2}$$

where $G = \begin{bmatrix} \boldsymbol{s}_1^T \\ \boldsymbol{s}_2^T \\ \vdots \\ \boldsymbol{s}_n^T \end{bmatrix}$ and $h = \begin{bmatrix} \sin\ a_1 \\ \sin\ a_2 \\ \vdots \\ \sin\ a_n \end{bmatrix}$.

In the presence of measurement errors, (2) is only valid approximately and one then seeks to minimize an error objective function or a least squares fit, based on the residual error, $G\boldsymbol{u} - h$. One obvious choice for this objective function is to account for an estimate of the error covariance matrix, Σ, associated with h (assuming the star GHA and Dec errors are insignificant in comparison). Given that $\boldsymbol{u}$ has a unit fixed norm, then finding an estimate of the navigator's geodetic coordinates is obtained through solving the following constrained minimization problem

$$\begin{aligned} &\min_{\boldsymbol{u}}\ (G\boldsymbol{u} - h)^T \Sigma^{-1}\ (G\boldsymbol{u} - h) \\ &\text{subject to}\ \|\boldsymbol{u}\|^2 = 1 \end{aligned} \tag{3}$$

which turns out to be an instance of the Trust Region Subproblem [8] with an equality constraint.

Put $F = G^T\Sigma^{-1}G$, $k = G^T\Sigma^{-1}h$ and $c = h^T\Sigma^{-1}h$, TRS problem (3) becomes

$$\begin{aligned} &\min_{\boldsymbol{u}} \ \boldsymbol{u}^T F\boldsymbol{u} - 2k^T\boldsymbol{u} + c \\ &\text{subject to } \|\boldsymbol{u}\|^2 = 1 \end{aligned} \tag{4}$$

where F is generally a positive definite 3×3 matrix. It becomes singular if and only if $rank\ G < 3$, which rarely occurs if G is a tall matrix. The Lagrangian associated with (4) is

$$\boldsymbol{\mathcal{L}}(\boldsymbol{u}, \lambda) \ = \ (\boldsymbol{u}^T F\boldsymbol{u} - 2k^T\boldsymbol{u} + c) + \ \lambda(\|\boldsymbol{u}\|^2 - 1)$$

and it is well known that an optimal solution of (4) is obtained if and only if (refer to [8][9])

$$\begin{aligned} &(F + \lambda I)\boldsymbol{u} = k \\ &\|\boldsymbol{u}\|^2 = 1 \\ &F + \lambda I \succcurlyeq \mathcal{O} \end{aligned} \tag{5}$$

It follows from [9] that the determinant of the 6×6 matrix

$$\widetilde{M}(\lambda) \triangleq \begin{bmatrix} -I & F + \lambda I \\ F + \lambda I & -kk^T \end{bmatrix}$$

vanishes for all the Lagrange multipliers satisfying the top two equations of (5). Finding the 6 Lagrange multipliers that satisfy $\det\big(\widetilde{M}(\lambda)\big) = 0$, is equivalent to solving the generalized eigenvalue problem,

$$\widetilde{M}(\lambda)\boldsymbol{y} = \ (M_o + \lambda M_1)\boldsymbol{y} = 0,$$

where $M_o = \begin{bmatrix} -I & F \\ F & -kk^T \end{bmatrix}$ and $M_1 = \begin{bmatrix} \mathcal{O} & I \\ I & \mathcal{O} \end{bmatrix}$. Most importantly an optimal solution of (4) is determined by the largest generalized eigenvalue, which is shown in [9] to be real. Let $\boldsymbol{y}$ be the associated generalized eigenvector and denote by $\boldsymbol{y}_1$ and $\boldsymbol{y}_2$, the vectors consisting of the top and bottom half entries of $\boldsymbol{y}$. It is shown in [9] that the solution, $\boldsymbol{u}$, reduces to

$$\boldsymbol{u} = \text{sign}(k^T\boldsymbol{y}_2)\frac{\boldsymbol{y}_1}{\|\boldsymbol{y}_1\|} \tag{6}$$

This method of determining, $\boldsymbol{u}$, is more stable than inverting the linear equation, $(F + \lambda I)\boldsymbol{u} = k$. Having specified M_o and M_1, as above, a Matlab (R2019a) implementation to solve (4) is given by the following three lines of code:

```
[y,lam] = eigs(M0,-M1,1,'largestreal');
y1 = y(1:3);
u = sign(k'* y(4:6))*y1/norm(y1);
```

Once the coordinates of $\boldsymbol{u}$ are determined, the Geodetic angles are given by $Lat = \sin^{-1} u_z$ and $Lon = -atan2(u_y, u_x)$ where $atan2(.,.)$ is defined as the 4-quadrant tangent inverse.

Assuming that the user is located on the ocean's surface, which is closely approximated by WGS84 ellipsoid, the user position on the ellipsoid follows as

$$x = (N + h)\cos Lat \cos Lon$$
$$y = (N + h)\cos Lat \sin Lon$$
$$z = ((1 - e^2)N + h)\sin Lat$$

where $h = 0$, $N = \frac{a}{\sqrt{1-e^2 sin^2 Lat}}$, $a = 6378137.0\,m$ and $e^2 \approx 0.00669437999 \ll 1$. The coordinates $[x, y, z]^T$ are given in the Earth-Centered, Earth-Fixed (ECEF) frame.

2.3 Example

Figure 2 uses star position data from [6] and shows LOPs corresponding to Deneb, Fomalhaut and Aldebaran around 3:00:00 UT on January 2, 1990. The ephemeris angles and measured altitudes are summarized in Table 1. As is clear from the figure, the three LOPs intersect approximately at the simulated true position, 21° 12' N and 157 ° 30' W, shown as a black square. Solving (4) results in the Geodetic coordinates, 21° 11.7' N and 157 ° 30.2' W, which are very close to those of the true position. The very small difference is due to the rounding error of altitude measurements in [6].

Star	Time (UT)	GHA	Dec	Altitude
Deneb	3:00:00	196° 13.7'	45 ° 14'.7 N	50 ° 15'
Fomalhaut	3:01:00	162 ° 28.1'	29 ° 40'.7 S	38 ° 54'
Aldebaran	3:02:00	78 ° 9 .1'	16 ° 29'.5 N	15 ° 32'

Table 1. Ephemeris data of three sightings of Deneb, Fomalhaut and Aldebaran, taken on January 1, 1990 at 17:00 Hawaiian Standard Time.

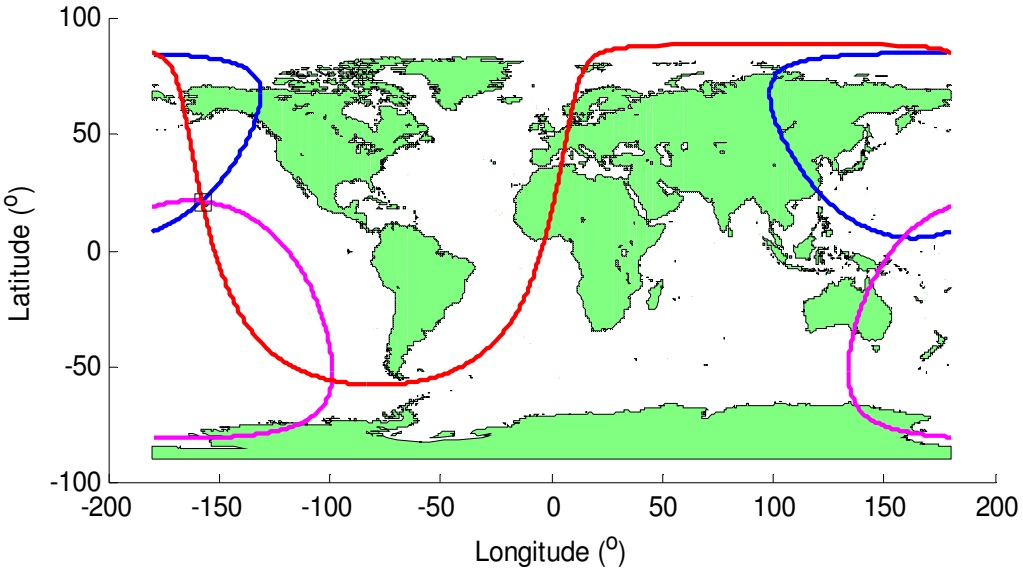

Figure 2. Lines of position associated with sightings occurring between UT 3:00:00 and 3:02:00 of Deneb (blue), Fomalhaut (magenta) and Aldebaran (red). The true user Geodetic position is 21° 12' N and 157 ° 30' W, shown as a black square.

3. CUED SIGHT REDUCTION

3.1 Problem Formulation

In this section it is assumed that one has some prior coarse knowledge of the navigator location. As illustrated in Figure 3, the region where the user resides is modelled by the linear inequality

$$e_x u_x + e_y u_y + e_z u_z \geq \beta, \quad (0 \leq \beta < 1) \tag{7}$$

which constrains the Geodetic unit vector, $\boldsymbol{u} \equiv [u_x, u_y, u_z]^T$, to point within an angle, not larger than $cos^{-1}\beta$ from the cone central axis, oriented along the unit vector, $[e_x, e_y, e_z]^T$.

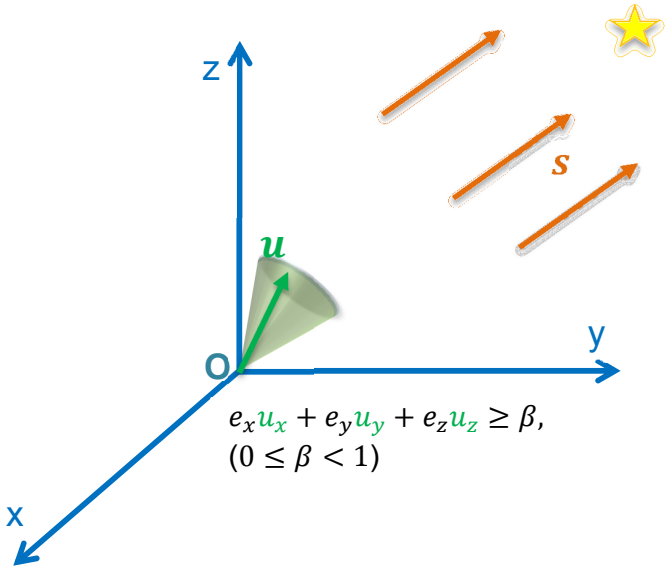

Figure 3. Cued sight reduction

Given the additional constraint (7), the optimization problem to be solved becomes

$$\begin{aligned} \min_{\boldsymbol{u}} \quad & \boldsymbol{u}^T F \boldsymbol{u} - 2k^T \boldsymbol{u} + c \\ \text{subject to} \quad & \|\boldsymbol{u}\|^2 = 1, \\ & e_x u_x + e_y u_y + e_z u_z \geq \beta \end{aligned} \tag{8}$$

The navigator's location may occur on the cone boundary, in which case the above inequality turns into an equality. If one then divides both sides of this equality by e_z, one obtains $u_z = \alpha - (a_x u_x + a_y u_y)$ where $a_x \equiv e_x/e_z$, $a_y \equiv e_x/e_z$ and $\alpha \equiv \beta/e_z$. This division operation, of course, assumes that the coefficient, e_z, of u_z in (7) is reasonably large in magnitude to avoid numerical problems. If this coefficient is zero or nearly zero, then one may switch to u_x or u_y, and divide by e_x or e_y, whichever is largest in magnitude. In the following a division by e_z, is assumed and as outlined above, this leads to the compact expression $u_z = \alpha - [a_x, a_y][u_x, u_y]^T$ where $\alpha = \beta/e_z$. Plugging this expression in (4) results in a lower dimension optimization problem, which turns out to be a Trust Region Subproblem with an equality constraint. In fact it can be shown that the new TRS problem (corresponding to cone boundary solutions) is

$$\min_{\mathbf{v}} \quad \mathbf{v}^T \check{F} \mathbf{v} + 2m^T \mathbf{v} \quad \text{subject to } \mathbf{v}^T B \mathbf{v} = \gamma^2 \tag{9}$$

where $\mathbf{v}$ is related to $[u_x, u_y]^T$ through the affine transformation, $\mathbf{v}=[u_x, u_y]^T - r$, with $r \equiv [r_x, r_y]^T = \alpha B^{-1} a$ and $a \equiv [a_x, a_y]^T$. The B matrix and the remaining parameters of problem (9) are summarized below:

$$B = I_2 + aa^T = \begin{bmatrix} 1 + a_x^2 & a_x a_y \\ a_x a_y & 1 + a_y^2 \end{bmatrix} \succ 0,$$

$\gamma = \sqrt{1 - \beta^2} > 0$, which is the sine of half the cone angle,

$$\check{F} = \begin{bmatrix} \check{F}_{11} & \check{F}_{12} \\ \check{F}_{12} & \check{F}_{22} \end{bmatrix} \text{ where } \begin{matrix} \check{F}_{11} = F_{33} a_x^2 - 2F_{13} a_x + F_{11} \\ \check{F}_{22} = F_{33} a_y^2 - 2F_{23} a_y + F_{22} \\ \check{F}_{12} = F_{33} a_x a_y - F_{23} a_x - F_{13} a_y + F_{12} \end{matrix},$$

$m = [p_x - p_z a_x, p_y - p_z a_y]^T$ with $p \equiv \left[p_x, p_y, p_z\right]^T = Fq - k$ and $q \equiv [r_x, r_y, \alpha - r^T a]^T$.

It follows from [9] that the determinant of the 4×4 matrix

$$\check{M}(\lambda) = \begin{bmatrix} -B & \check{F} + \lambda B \\ \check{F} + \lambda B & -mm^T/\gamma^2 \end{bmatrix}$$

vanishes for all Lagrange multipliers associated with problem (9). An optimal solution of (9) can be determined using

$$\mathbf{v} = -\gamma \, \text{sign}(m^T \boldsymbol{y}_2) \frac{\boldsymbol{y}_1}{\|\boldsymbol{y}_1\|_B} \tag{10}$$

where, as explained in [9], $\boldsymbol{y}_1$ and $\boldsymbol{y}_2$ are the first and second half components of the eigenvector, $\boldsymbol{y}$, associated with the largest eigenvalue (real) of $\check{M}(\lambda)$. The norm, $\|\boldsymbol{y}_1\|_B$ is $\sqrt{\boldsymbol{y}_1^T B \boldsymbol{y}_1}$. Once an optimal solution, $\mathbf{v}$ of (9) is found, $\boldsymbol{u}$ can be determined using $[u_x, u_y]^T = \mathbf{v} + r$ and $u_z = \alpha - [a_x, a_y][u_x, u_y]^T$.

A general algorithm to solve (8) is summarized below

---

1. Find all local minima of (4). This is equivalent to computing all real generalized eigenvalues of $(M_o + \lambda M_1)\boldsymbol{y} = 0$, where $M_o = \begin{bmatrix} -I & F \\ F & -kk^T \end{bmatrix}$ and $M_1 = \begin{bmatrix} \mathcal{O} & I \\ I & \mathcal{O} \end{bmatrix}$ are 6×6 matrices.
2. Only keep the real eigenvalues, λ, whose corresponding solutions, $\boldsymbol{u} = (F + \lambda I)^{-1} k$, satisfy the inequality constraint (7) and store these eigenvalues (if any) in an array. If the eigenvalue array remains empty, then move to step 5.
3. If the largest real eigenvalue is one of the stored eigenvalues, then stop.
4. Compute the objective function, $\boldsymbol{u}^T F \boldsymbol{u} - 2k^T \boldsymbol{u}$, for each eigenvalue in the array.
5. Solve (9) by computing the largest generalized eigenvalue of $\left(\check{M}_o + \lambda \check{M}_1\right)\boldsymbol{y} = 0$, where $\check{M}_o = \begin{bmatrix} -B & \check{F} \\ \check{F} & -mm^T/\gamma^2 \end{bmatrix}$ and $\check{M}_1 = \begin{bmatrix} \mathcal{O} & B \\ B & \mathcal{O} \end{bmatrix}$ are 4×4 matrices.
6. Apply (10) to compute the optimal solution, $\mathbf{v}$, of (9) and then determine $\boldsymbol{u}$ as $[u_x, u_y]^T =$

$\mathbf{v} + r$ and $u_z = \alpha - [a_x, a_y][u_x, u_y]^T$. Finally compute the associated objective function value, $\boldsymbol{u}^T F \boldsymbol{u} - 2k^T \boldsymbol{u}$.

7. If the eigenvalue array of step 2 is empty, then return $\boldsymbol{u}$ of step 6 and stop. Otherwise select $\boldsymbol{u}$ that results in the lowest objective value in steps 4 and 6, then stop.

Once the coordinates of $\boldsymbol{u}$ are determined, the Geodetic angles follow as $Lat = \sin^{-1} u_z$ and $Lon = -atan2(u_y, u_x)$.

3.2 Example

Figure 4 is an illustration of the constrained sight reduction positioning problem using the star position data of Table 1. The shown black curve delimits the region where the user is thought to be. This cue region is about 2^o across. In this figure the region center coincides with the true position, 21° 12' N and 157 ° 30' W, depicted as a black star. By artificially injecting large errors to the computed true star altitudes, the geolocation fix obtained by solving (4), is shown as a blue circle, and is clearly displaced beyond the cue region. However, implementing the above algorithm to solve (8), forces the inequality constraint (7) to become active (i.e. turn into an equality constraint), and consequently prevents the optimal solution from occurring outside the cue region. The optimal solution is shown as a red square and lies on the cue boundary, close to the LOP intersection region. Had the altitude errors been much smaller, the inequality constraint would not turn active and the optimal solution would lie inside the cue region. The diamond blue marker corresponds to the optimal solution of (4), when the diagonal of the weight matrix, Σ, is populated with the cosine squared of the altitudes [7], and zero elsewhere. Clearly this weighting strategy tends to align the optimal fix with the center of the LOP intersection region.

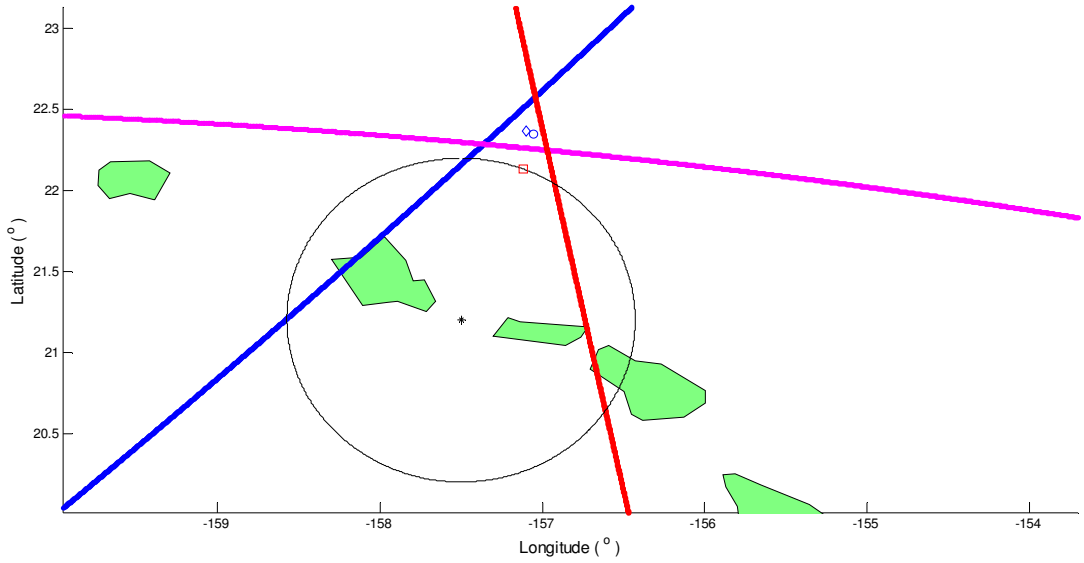

Figure 4. Cued sight reduction positioning. The cue region constraint is given by (7) assuming $cos^{-1}\beta = 1^o$.

4. COMPUTER SIMULATIONS

The same celestial position data given in Table 1 are used for the Monte Carlo simulations of this section. The true user position is again 21° 12' N and 157 ° 30' W. Figure 5 shows the

North-East localization errors in nautical miles, incurred when the three star altitudes are contaminated with additive zero mean Guassian errors ($\sigma = 2'$). A total of 10000 noisy altitude realizations are simulated to generate the user position error cloud of Figure 5. The plotted errors correspond to the position deviation of the solution of (4) from the true user position. No special weighting is applied to the altitude measurements (i.e. Σ is the identity matrix).

More simulations were carried out experimenting with different levels of altitude measurement error. For each measurement error, 10000 Monte Carlo simulations are executed to generate a position error cloud, similar to that shown in Figure 5. A distance root mean square error is then computed and entered in the second column of Table 2. The rms error clearly increases, almost linearly, with increasing altitude error, σ. The last column contains the lowest distance errors obtained from deriving the CRLB (Cramer-Rao Lower Bound).

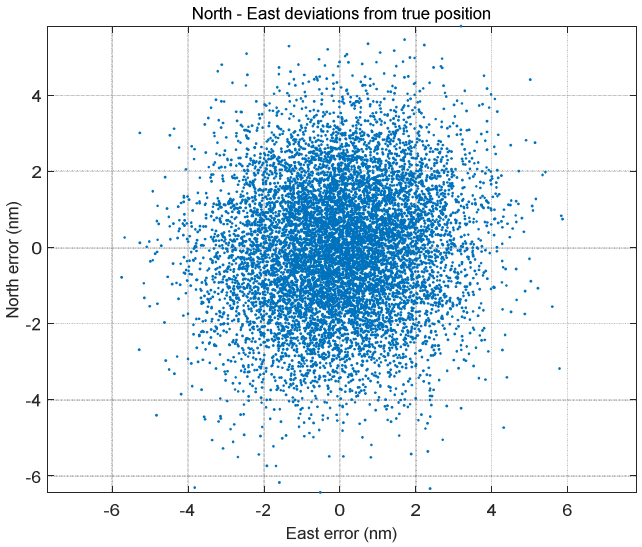

Figure 5. Position errors in nautical miles associated with 10000 altitude error realizations, $\sigma = 2'$.

It is clear from Table 2 that sub-nautical mile geolocation accuracy is possible, provided that accurate and numerous altitude measurements are taken. To achieve this it is required that six or more mid-altitude planets/stars are sighted along different directions around the navigator. This necessitates the automation process of star sighting and altitude (or zenith distance) measurement, to ensure that measurements are collected accurately and simultaneously. This last requirement is of particular importance to moving platforms and airborne vehicles. Note that for airborne vehicles, the height above WGS84 ellipsoid, has to be measured independently (e.g. using a barometric altimeter).

Altitude error (arc minutes)	Distance Error (nm)	Lowest distance error (nm)
1	1.18	1.17
2	2.37	2.33
4	4.74	4.66
10	11.91	11.66
30	35.80	34.98
60	71.77	69.96

Table 2. Geolocation distance errors from true position in nautical miles

An important future research topic is the analysis of optimal star direction geometry to achieve the most accurate user localization. Bowditch [4] gave some clues on how to select star sightings, but more rigorous analysis is needed in this respect. Another research direction of interest to navigation in a GPS denied environment, is to combine star sight measurements with other types of measurements, such as distance measurements to beacons of known location.

5. CONCLUSIONS

In this paper a novel algorithm for solving the self-localization problem based on celestial sight reduction is presented. The localization method relies on sightings of several celestial bodies and measurements of their altitudes in the sky. The proposed solving approach is based on the Trust Region Subproblem (TRS) formulation, whose solution is obtained in closed-form through generalized eigen-decomposition. The first part of the paper shows how a closed-form solution is established through the computation of the largest eigenvalue. The second part of this work focusses on constrained self-localization, which requires an additional linear inequality constraint to be accounted for in the original TRS formulation. A detailed algorithm to solve this new problem is provided and relies on solving two related TRS problems. The last part of the paper presents Monte Carlo simulations of the proposed solving approach as a function of altitude error. The outcome of these simulations provides good insight into the localization accuracy achievable using celestial sight reduction. Recommendations related to how to increase positioning accuracy are also given.

REFERENCES

[1] Kopp C., Milestones: Stellar Navigation to Satellite navigation, *Defence Today,* Vol.6.No.2, 2007

[2] Admiralty: The Nautical Almanac, Her Majesty's Nautical Almanac Office, UK Hydrographic Office, 2020

[3] Umland, H., A Short Guide to Celestial Navigation, Website: https://celnav.de, 2019

[4] Bowditch, N., American Practical Navigator, National Geospatial-Intelligence Agency, 2019.

[5] Tsou, Ming-Cheng, Celestial Navigation Fix Based on Particle Swarm Optimization, *Polish Maritime Research*, Vol. 22, 2015

[6] Metcalf, T. R. and Metcalf, F. T., On the Overdetermined Celestial Fix, *Navigation*, Vol. 38, 1991

[7] Metcalf, T. R., An Extension to the Overdetermined Celestial Fix, *Navigation*, Vol. 39, 1992

[8] Conn, A. R., Gould N. I. M., and Toint, P. T., Trust-Region Methods, MPS/SIAM Series on Optimization, 2000

[9] Adachi, S., Iwata, S., N. Yuji and Takeda, T., "Solving the Trust Region Subproblem by a Generalized Eigenvalue Problem", *Mathematical Engineering Technical Report, METR 2015-14*, April 2015